

## EFFECT OF OILS, SURFACTANTS AND COSURFACTANTS ON PHASE BEHAVIOR AND PHYSICOCHEMICAL PROPERTIES OF SELF-NANOEMULSIFYING DRUG DELIVERY SYSTEM (SNEDDS) FOR IRBESARTAN AND OLMESARTAN

ALI NASR<sup>1,\*</sup>, AHMED GARDOUH<sup>2</sup>, HASSAN GHONAIM<sup>2</sup>, ELSAYED ABDELGHANY<sup>1</sup>, MAMDOUH GHORAB<sup>2</sup>

<sup>1</sup>Department of Pharmaceutics, Faculty of Pharmacy and Pharmaceutical Industries, Sinai University, Alarish, Egypt, <sup>2</sup>Department of Pharmaceutics, Faculty of Pharmacy, Suez Canal University, Ismailia, Egypt  
Email: ali.nasr@su.edu.eg

Received: 28 Sep 2015, Revised and Accepted: 30 Nov 2015

### ABSTRACT

**Objective:** The main purpose of this study was to optimize the different conditions for the preparation of self-nanoemulsifying drug delivery system (SNEDDS) for both Irbesartan (IRB) and Olmesartan (OLM).

**Methods:** Based on solubility study and emulsification efficiency, Preliminary investigations of various oils, surfactants and cosurfactants were carried out for selection of the proper SNEDDS ingredients. Pseudoternary phase diagrams were then plotted using series of concentrations to obtain optimum SNEDDS components that identify the efficient self-nanoemulsifying region. Sixteen unloaded SNEEDS formulae were prepared using Capryol 90, Cremophor RH 40 and Transcutol HP as oil, surfactant and cosurfactant respectively. The prepared SNEDDS were evaluated for self-nanoemulsification time, the effect of dilution (with different volumes at different pH values), optical clarity, viscosity, droplet size analysis as well as the polydispersity index (PDI). SNEDDS formulae were also evaluated for thermodynamic stability and zeta potential to confirm the stability of the prepared SNEDDS.

**Results:** The results showed that the mean droplet size of all reconstituted SNEDDS was found to be in the nanometric range (<100 nm) and showed optimum PDI values. All formulae also showed rapid emulsification time, good optical clarity and found to be highly stable. Formulae with the smallest particle size, lowest emulsification time, best optical clarity and robust to dilution and pH change were selected to be loaded with IRB and OLM for further study.

**Conclusion:** It was concluded that the prepared self-emulsified prototype was ready to incorporate many poorly soluble drugs in order to improve their solubility as well as bioavailability profile.

**Keywords:** Irbesartan, Olmesartan, Self-nanoemulsifying drug delivery system (SNEDDS), Capryol 90, Cremophor RH 40 and Transcutol HP.

© 2016 The Authors. Published by Innovare Academic Sciences Pvt Ltd. This is an open access article under the CC BY license (<http://creativecommons.org/licenses/by/4.0/>)

### INTRODUCTION

In the drug discovery, Most of the new drug candidates and many existing drug molecules show poor aqueous solubility which leads to poor oral bioavailability, high intra- and inter-subject variability and lack of dose proportionality [1]. The greatest challenge is to present the poorly water-soluble drugs into orally administered medications with sufficient bioavailability. To increase the oral bioavailability of poorly water soluble drugs, various formulation strategies have been adopted including the use of cyclodextrins, nanoparticles, solid dispersions, permeation enhancers and lipid-based formulations [2].

In recent years, considerable attention has been focused on lipid-based formulations to improve the oral bioavailability of poorly water-soluble and lipophilic drugs. In fact, the most popular strategy is the incorporation of the drug molecule into inert lipid vehicles such as oils and surfactant dispersions, self-emulsifying formulations, emulsions, and liposomes with particular emphasis on self-nanoemulsifying drug delivery systems (SNEDDS) [3]. Self-nanoemulsifying drug delivery systems (SNEDDS) are isotropic and thermodynamically stable mixtures of oil, surfactant, cosurfactant and drug that have a novel property of forming fine oil-in-water (o/w) nanoemulsion in the nanometric range (10-100 nm) when introduced into the aqueous phase under gentle agitation [4]. Upon administration, the isotropic mixture will come in contact with the aqueous phase of gastrointestinal tracts and form an oil-in-water nanoemulsion with the aid of gastrointestinal motility. This spontaneous formation of nanoemulsion in the gastrointestinal tract presents the drug in a solubilized form, in small droplets of oil, all over its transit through the GIT [5]. The nano-sized droplets provide a large interfacial surface area for drug release and absorption. Apart from solubilization, the presence of oily phase in the formulation helps improve bioavailability by affecting the drug absorption [6]. Selection of a suitable self-nanoemulsifying

formulation depends mainly upon the assessment of drug solubility in various components, the area of the self-nanoemulsifying region obtained in the phase diagram, and the droplet size of the resultant emulsion following self-emulsification [7]. Finally, SNEDDS offer the opportunity to deliver poorly water soluble drugs to the gastrointestinal tract in a dissolved state which leads to avoiding the dissolution step (which can limit the absorption rate of lipophilic drugs), reduction in inter- and intra-subject variability, reduction of food effect and ease of manufacturing and scale-up [8].

Both Irbesartan (IRB) and Olmesartan (OLM) are novel selective angiotensin II receptor blockers that are approved for the treatment of hypertension [9-10]. IRB is practically insoluble in water due to its hydrophobic nature as shown in fig. (1). The estimated bioavailability of IRB is greater than 60%; however plasma level do not increase proportionally with dose. The calculated biopharmaceutical parameter suggests that IRB has a very low absorbable dose. Also the volume of aqueous medium required to dissolve the highest dose, calculated using ratio of dose/solubility was 20L. Thus, theoretically, IRB exhibits a solubility limited bioavailability and would be advantageous to enhance solubility and dissolution rate of IRB [11]. On the other hand, OLM is also poorly water soluble drug and its aqueous solubility is reported to be less than 1 mg/ml as presented in fig. (2). It is a prodrug that is rapidly de-esterified during absorption from the gastrointestinal tract to produce an active metabolite. The oral bioavailability of OLM is only 26% in healthy humans due to low solubility in water and unfavorable breakage of the ester drug to a poorly permeable parent molecule in the gastrointestinal fluids [12]. To overcome these problems concerning IRB and OLM there was a need to develop SNEDDS which improves the oral bioavailability of both drugs. The main objective of this research was to optimize the different conditions for the preparation of self-nanoemulsifying drug delivery system (SNEDDS) for both IRB and OLM to enhance their oral bioavailability.

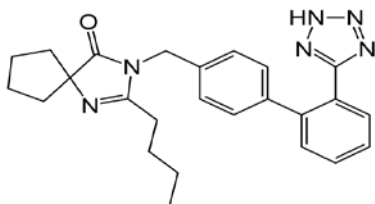


Fig. 1: Chemical Structure of Irbesartan

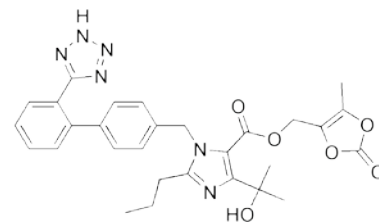


Fig. 2: Chemical Structure of Olmesartan

## MATERIALS AND METHODS

### Materials

Irbesartan, Miglyol 812 (Caprylic/Capric Triglyceride), Miglyol 818 (Caprylic/Capric/linoleic Triglyceride), Miglyol 829 (Caprylic/Capric/Succinic Triglyceride) and Labrafil M 1944 CS (Oleoyl polyoxy-6 glycerides) (gift from Medical Union Pharmaceuticals, Egypt), Olmesartan (Jedco International Pharmaceuticals, Egypt), Capryol 90 (Propylene glycol monocaprylate), Gelucire 44/14 (Lauroyl polyoxy-32 glycerides), Lauroglycol FCC (Propylene glycol laurate), Labrafac lipophile WL 1349 (Caprylic/Capric Triglyceride), Maisine 35-1 (Glyceryl Linoleate) and Transcutol HP (2-(2-Ethoxyethoxy)ethanol) (Gattefossé, France), Cremophor RH40, Cremophor S9 and Labrasol (Nerol Chemicals, Egypt), Bitter almond oil, Castor oil, Olive oil, Cotton seed oil, Arachis oil, Oleic acid, Hydrochloric acid and Propylene Glycol (El Nasr Pharmaceutical Chemicals, Egypt), Tween 20, Tween 40, Tween 60, Tween 80, Span 20, Span 80, PEG 400, PEG 600 and Sodium Hydroxide (Oxford Laboratory, India), PEG 200 (Loba Chem. Pvt. Ltd., India), Glycerin (El Gomhouria Pharmaceuticals, Egypt) and Sodium Dihydrogen Phosphate (PureLab, USA). Other chemicals are of HPLC grade.

### Methods

#### Preformulation study (Selection of SNEDDS components)

#### Study of IRB and OLM solubility in various oils, surfactants and cosurfactants

In order to find out the proper SNEDDS components with good solubilizing capacity for both IRB and OLM, saturation solubility of both drugs was carried out in different oils (Gelucire 44/14, Lauroglycol FCC, Labrafac lipophile WL 1349, Capryol 90, Labrafil M 1944 CS, Miglyol 812, Miglyol 818, Miglyol 829, Maisine 35-1, Bitter almond oil, Castor oil, Olive oil, Cotton seed oil, Arachis oil and Oleic acid), surfactants (Cremophor RH 40, Cremophor S 9, Labrasol, Tween 20, Tween 40, Tween 60, Tween 80, Span 20 and Span 80) and cosurfactants (Transcutol HP, PEG 200, PEG 400, PEG 600, Propylene glycol and Glycerin) using shake flask method [13]. In this study, an excess amount of the drug (approximately 500 mg) was introduced into 2 ml of each vehicle in screw capped greiner tubes. The mixtures were mixed well using a vortex mixer (Maximix II, USA) for 10 min to enhance the proper mixing of the drug with the vehicles and thus facilitate the solubilization. The obtained mixtures were then shaken for 72 h in an isothermal mechanical shaker (Clifton shaking water bath, UK) maintained at 40 °C to attain equilibrium. After reaching equilibrium, the equilibrated samples were centrifuged at 3000 r. p. m for 15 min to precipitate the undissolved IRB and OLM. Aliquots from the supernatants were then withdrawn and filtered through a membrane filter (0.45 µm, Whatmann). Filtered solutions were suitably diluted with methanol, and drug concentrations were determined using Hitachi UV-Vis spectrophotometer (Hitachi, Japan) at  $\lambda_{\max}$  246 nm for IRB and 256 nm for OLM [14]. All measurements were done in triplicate, and the solubility was expressed as the mean value (mg/ml)±SD.

#### Preliminary screening of surfactants for emulsification efficiency

Different surfactants (Cremophor RH 40, Cremophor S 9, Labrasol, Tween 20, Tween 40, Tween 60, Tween 80, Span 20 and Span 80) were screened for its emulsification ability in the selected oily phase. Surfactant selection was done on the basis of transparency

percentage and ease of emulsification [15]. Briefly, 500 µl of each surfactant was added to 500 µl of the selected oil. The mixtures were gently heated at 50°C for 2 min to attain homogenization of components. From each mixture, 100 µl were then diluted with distilled water up to 50 ml in glass stoppered flask. The stoppered flasks were inverted several times and the number of flask inversions required to form a homogenous nanoemulsion (with no turbidity or phase separation) was counted. Furthermore, the formed emulsions were allowed to stand for 2 h and their percentage of transmittance was assessed at 650 nm (by means of UV-Vis Spectrophotometer) using distilled water as blank. The percentage of transmittance was calculated for each emulsion in triplicates and the average values±SD were calculated. The surfactant forming a clear emulsion with fewer inversions and a higher percentage of transmittance was selected [16].

#### Preliminary screening of cosurfactants for emulsification efficiency

The selected oily phase and surfactant were used for further screening of the different cosurfactants (Transcutol HP, PEG 200, PEG 400, PEG 600, Propylene glycol and Glycerin) for their emulsification efficiency. Mixtures of 200 µl of co-surfactant, 400 µl of selected surfactant and 600 µl of selected oil were prepared and evaluated in the same manner as described in preliminary screening of surfactants [17].

#### Construction of pseudo ternary phase diagram

In order to determine the concentration of components for the existing range of the SNEDDS, a pseudo ternary phase diagram was constructed at ambient temperature using a water titration method [18]. Oil, surfactant and cosurfactant were grouped in different combinations for phase studies. Surfactant and co-surfactant (Smix) in each group were mixed in different weight ratio (1:0, 1:1, 1:2, 1:3, 2:1 and 3:1). These Smix ratios were chosen in increasing concentration of surfactant with respect to cosurfactant and in increasing the concentration of cosurfactant with respect to surfactant. For each phase diagram, oil and specific Smix ratio are mixed thoroughly in different weight ratios (1:9, 1:7, 1:5, 1:4, 1:3, 1:2, 1:1 and 2:1) in different glass vials. Different ratios of oils and Smix were made to delineate the boundaries of phase precisely [19]. The amount of aqueous phase was incremented by 5% to provide a concentration of aqueous phase in the range of 5–95% of total volumes. After each addition of aqueous phase, the mixtures in the vials were vortexed for 2 min and allowed to equilibrate. The change in physical states from transparent to turbid and vice-versa were visually observed and marked on the three component ternary phase diagram where each axis represented the oil, Smix and water, respectively. The different phase diagrams were plotted using CHEMIX ternary plot software (CHEMIX School Ver. 3.60, Pub. Arne Standnes).

#### Preparation of unloaded SNEDDS

Once the self-nanoemulsifying area was identified, SNEDDS formulae with desired component ratios were prepared. The ratio of surfactant to cosurfactant (Smix) was also optimized using pseudo ternary phase diagrams. A series of unloaded SNEDDS formulae were prepared with varying weight ratios of selected oil (5–15% w/w) and Smix (20–80% w/w) as presented in table (1). The ingredients were accurately weighed and mixed in stoppered glass vials using a vortex mixer to ensure complete mixing. These systems were warmed to 40 °C using a water bath for 30 min with mild shaking until a clear solution was obtained. The prepared formulae were then stored at room temperature until further use [20].

**Table 1: Percent w/w compositions of optimized unloaded SNEDDS formulae**

Formula	Oil (% w/w)	Smix (% w/w)
F1	5	20
F2	5	40
F3	5	60
F4	5	80
F5	8.5	20
F6	8.5	40
F7	8.5	60
F8	8.5	80
F9	11.5	20
F10	11.5	40
F11	11.5	60
F12	11.5	80
F13	15	20
F14	15	40
F15	15	60
F16	15	80

**Characterization and evaluation of unloaded SNEDDS****Robustness to dilution**

In order to simulate *in vivo* dilution behavior, the effect of dilution on emulsion characteristics was studied. Robustness of different SNEDDS formulae to dilution was done by diluting 1 ml of each formula 10, 100 and 1000 times with distilled water, 0.1 N HCL and phosphate buffer of pH 6.8. The diluted systems were mixed using a magnetic stirrer at 37 °C to simulate body temperature and gastric motility in the gastrointestinal tract till complete homogeneity. These systems were stored at ambient temperature for 24 h then visually observed for any signs of phase separation [21].

**Thermodynamic stability studies**

The prepared SNEDDS formulae were subjected to heating-cooling cycles, centrifugation, and freeze-thaw cycles, where the physical appearances of the formulae were visually observed at the end of each testing. In heating cooling cycles, the prepared formulae were subjected to six cycles between refrigerator temperature 4 °C and 45 °C with storage at each temperature for 48 h. The formulae that did not show any phase separations, creaming or cracking were subjected to centrifugation at 3500 rpm for 30 min. Finally, only formulae which passed the previous two steps were stored at alternating temperatures of -21 °C and 25 °C, with the duration of 48 h at each temperature, for three cycles [22].

**Assessment of efficiency of self-emulsification (Dispersibility test)**

The self-emulsification efficiency of SNEDDS was assessed using a standard USP dissolution apparatus type II. 1 ml of each formula was added to 500 ml of distilled water maintained at 37±0.5 °C. Gentle agitation was provided by a standard stainless steel dissolution paddle rotating at 50 rpm. The lipid-based formulations were assessed visually according to the rate of emulsification and final appearance of the emulsion. The *in-vitro* performance of the formulation was visually evaluated using the following grading system [23].

Grade A: Rapidly forming an emulsion having a clear or bluish appearance (within 1 minute).

Grade B: Rapidly forming, slightly less clear emulsion, having a bluish-white appearance.

Grade C: Fine milky emulsion that formed within 2 min.

Grade D: Dull, a grayish white emulsion having a slightly oily appearance that is slow to emulsify (longer than 2 min).

Grade E: Formulation, exhibiting either poor or minimal emulsification with large oil globules present on the surface.

**Self-emulsification time**

In this test, a predetermined volume of each formula (1 ml) was introduced into 300 ml of distilled water maintained at 37±0.5 °C in

a glass beaker and the contents mixed gently using a magnetic stirrer rotating at constant speed. The emulsification time (the time required for a pre-concentrate to form a homogeneous mixture upon dilution) was monitored by visually observing the disappearance of SNEDDS and the final appearance of the nanoemulsion [24].

**Viscosity determination**

The viscosity of the prepared SNEDDS formulae was measured at 25±0.5 °C as such before and after dilution by Brookfield viscometer (Brookfield Engineering Labs, USA) using spindle CC3-14 with shear rate at 100 rpm [25].

**Spectroscopic characterization of optical clarity**

The percentage transmittance as measurements of optical clarity for the prepared SNEDDS formulae was measured spectrophotometrically using Hitachi UV-Vis spectrophotometer (Hitachi, Japan) after dilution with water. The SNEDDS formulae were 100 times diluted with distilled water and analyzed at 650 nm using distilled water as the standard blank solution [26].

**Transmission electron microscopy (TEM)**

The surface morphology and globule size of the prepared SNEDDS formulae were observed using Transmission electron microscopy (JEM-2100, USA). Prior to analysis, the SNEDDS samples were diluted 10 times with distilled water. A drop from the resultant nanoemulsion was deposited on a film-coated copper grid forming a thin liquid film. The films were then negatively stained with 2% (w/v) phosphotungstic acid solution. After air drying, the stained films were photographed by transmission electron microscopy [27].

**Droplet size analysis and poly dispersibility Index (PDI) determination**

The droplet size is an important factor in self-emulsification performance because it determines the rate and extent of drug release as well as absorption. Prior to measurement, 1 ml of each SNEDDS formula was diluted 10 times with distilled water. The globule size and poly dispersibility index of the formed nanoemulsions were determined by dynamic light scattering (DLS) using a photon correlation spectrometer (Zetasizer, Malvern Instruments LTD, UK) which analyzes the fluctuations in light scattering due to the Brownian motion of the particles. Light scattering was monitored at 25 °C at scattering angle 90 ° [28].

**Zeta potential determination**

The zeta potential of the diluted SNEDDS formulae was determined using Zetasizer (Malvern Instruments, UK). Samples were placed in clear disposable zeta cells and results were recorded. The charge on emulsion droplets and their zeta potential values were obtained [28].

**RESULTS AND DISCUSSION****Preformulation study (Selection of SNEDDS components)****Study of IRB and OLM solubility in various oils, surfactants and cosurfactants**

Solubility studies were aimed at identifying suitable SNEDDS components that possess the good solubilizing capacity for both IRB and OLM. Identifying the suitable oil, surfactant and cosurfactant having the maximal solubilizing potential for drugs under investigation is very important to achieve optimum drug loading [29]. Oils can solubilize the lipophilic drug in a specific amount so they are the main excipients because they can increase the fraction of lipophilic drug transported via the intestinal lymphatic system, thereby increasing absorption from the GI tract. Capryol 90 was selected as an oily phase for both drugs due to its highest solubilization (176.47±5.48 mg/ml) for IRB and (164.69±3.59 mg/ml) for OLM compared to other screened oils as shown in fig. (3&6). Various non-ionic surfactants which cover wide HLB range may be used in combination with lipid excipients to promote self-emulsification. Surfactants form a layer around the emulsion droplets and hence reduce the interfacial energy, as well as provide a mechanical barrier to coalescence. This can prevent precipitation of the drug within the GI lumen and enhance prolonged existence of

drug molecules. Among the various surfactants screened, Cremophor RH 40 showed the best solubilizing potential for IRB ( $261.74 \pm 6.18$  mg/ml) as illustrated in fig. (4). However concerning OLM solubility in various surfactants, Labrasol exhibited a good solubilizing potential ( $241.51 \pm 6.28$  mg/ml) as shown in fig. (7). Transient negative interfacial tension and a fluid interfacial film are rarely achieved with the use of a single surfactant, usually necessitating the addition of a cosurfactant. The presence of cosurfactants decreases the bending stress of the interface and allows an interfacial film with sufficient flexibility to assume

different curvatures required to form a nanoemulsion over a wide range of compositions. Hence, the use of cosurfactant stabilizes the formed nanoemulsion. Among the solubility data in different cosurfactants, Transcutol HP exhibited maximum solubility for both IRB ( $287.56 \pm 6.67$  mg/ml) and OLM ( $299.96 \pm 2.98$  mg/ml) as presented in fig. (5&8). Similar results were obtained by Urvashi *et al.*, who found that the optimized components for lovastatin SNEDDS are Capryol 90 as oil, Cremophor RH 40 as a surfactant and Transcutol HP as cosurfactant [30].

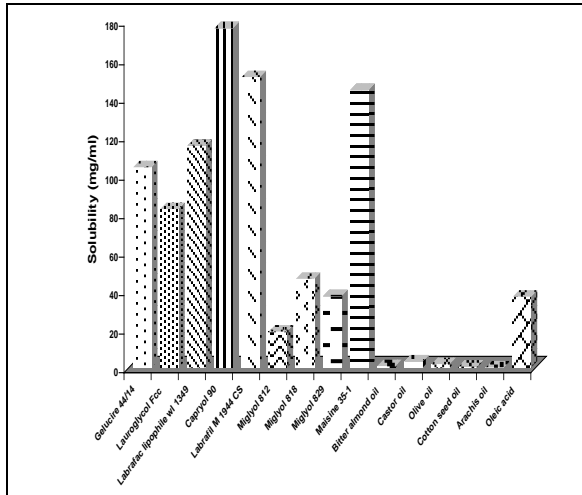


**Fig. 3: Solubility of IRB in various oils**

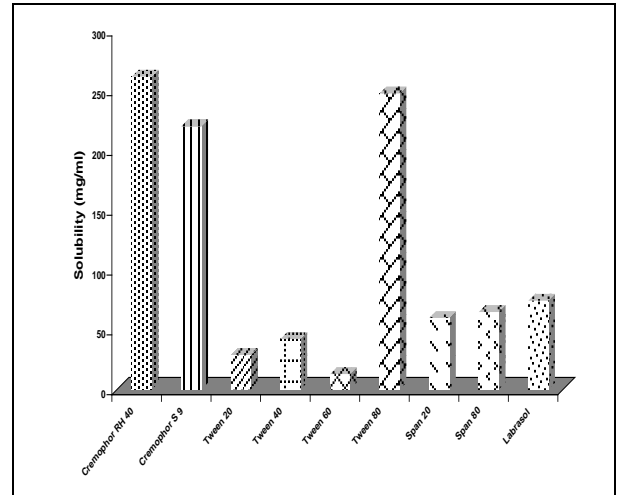


**Fig. 4: Solubility of IRB in various surfactants**

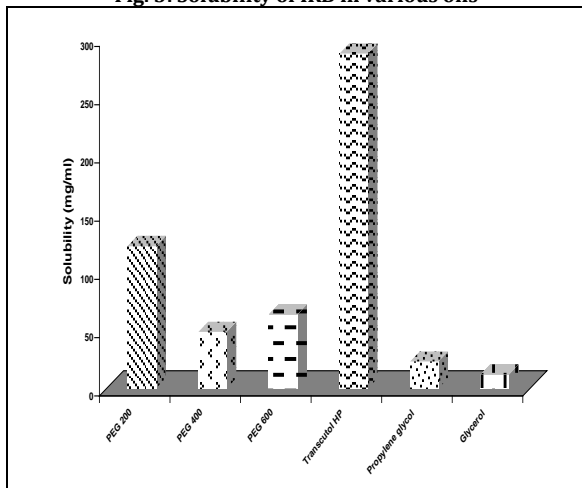


**Fig. 5: Solubility of IRB in various cosurfactants**

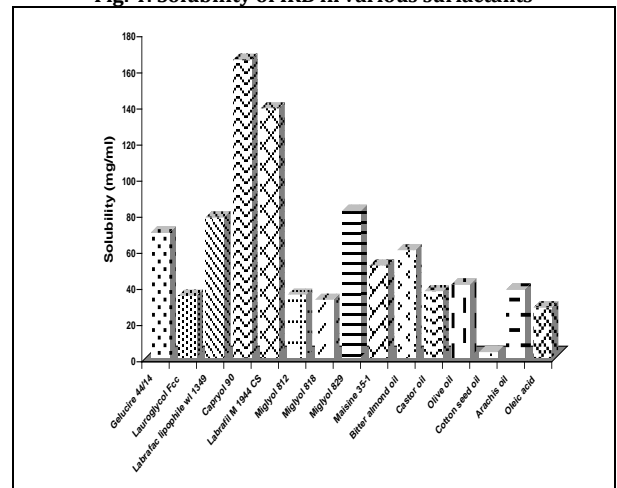


**Fig. 6: Solubility of OLM in various oils**

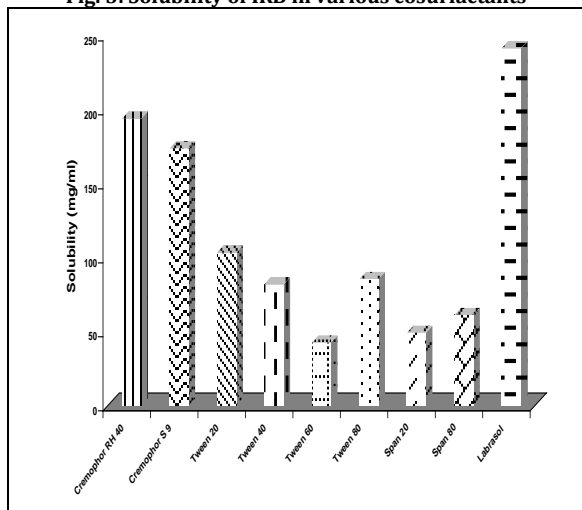


**Fig. 7: Solubility of OLM in various surfactants**

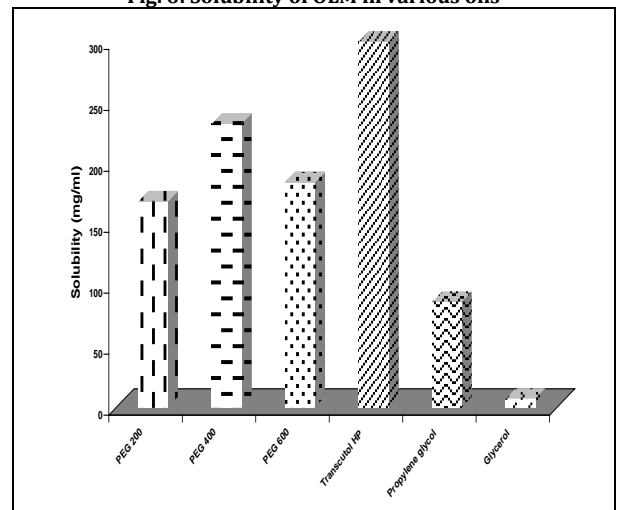


**Fig. 8: Solubility of OLM in various cosurfactants**

### Preliminary screening of surfactants for emulsification efficiency

If the surfactant or cosurfactant is contributing in drug solubilization, there could be a risk of precipitation of drug in the GI tract, as dilution of nanoemulsion will lead to lowering of the solvent capacity of the surfactant or cosurfactant [5]. Therefore, selection of the surfactant and cosurfactant in the further study was governed by their emulsification efficiency rather than their ability to solubilize IRB and OLM. Optical clarity corresponds to high transmittance, as opalescent dispersions will scatter incident radiation to a larger extent as compared to transparent dispersions. The intensity of light passing through such dispersion is attributed to the scattering of light which occurs due to the absence of optical homogeneities in the medium [4]. Hence, % transmittance could directly be used to

predict relative droplet size of the emulsion. Based on this principle, aqueous dispersions with high transmittance (lower absorbance) were considered optically clear and oil droplets were thought to be in a state of nanodispersion [31]. It was necessary to identify the combinations of surfactants and lipophiles that could produce stable SNEDDS. The transmittance percentage values of various dispersions are listed in the table (2). Emulsification studies clearly distinguished the ability of various surfactants to emulsify Capryol 90. The results revealed that Cremophor RH40 showed maximum transmittance (99.47±0.12%) and 4 inversions; whereas Labrasol formed a coarse emulsion with a white appearance (44.87±0.95%), when it was mixed with Capryol 90. Amongst the surfactants studied, Cremophor RH40 has high HLB number 14-15 compared to other surfactants used. Thus, Cremophor RH40 was chosen as a surfactant for further investigation due to its better nanoemulsification efficiency.

**Table 2: Emulsification efficiency of various surfactants**

Surfactants	% Transmittance*	No. of inversions
<b>Cremophor RH 40</b>	<b>99.47±0.12</b>	<b>4</b>
Cremophor S 9	14.90±0.66	17
Tween 20	98.17±0.40	5
Tween 40	80.97±1.01	11
Tween 60	74.93±0.35	9
Tween 80	97.60±0.26	15
Span 20	52.67±0.75	17
Span 80	56.57±0.50	13
Labrasol	44.87±0.95	7

\*Values are expressed as mean±SD, n=3

### Preliminary screening of cosurfactants for emulsification efficiency

Interestingly, all the hydrophilic cosurfactants employed appeared to improve the emulsification ability of Capryol 90 and Cremophor RH 40. It is well documented that negative interfacial tension and fluid interfacial film is rarely achieved by the use of a single surfactant, usually necessitating the addition of a cosurfactant. The presence of cosurfactants decreases the bending stress of interface and allows the interfacial film sufficient flexibility to acquire different curvatures required to form nanoemulsion over a wide range of compositions. The addition of a cosurfactant to the surfactant-containing formulation was reported to improve the

dispersibility and drug absorption from formulation [32]. As depicted in table (3), Transcutol HP exhibited good emulsification efficiency with Capryol 90 and Cremophor RH 40 mixture, showing maximum transmittance (99.83±0.06%) and 3 inversions only compared to other employed cosurfactants. It was cleared that all the employed cosurfactants appeared to improve the emulsification ability of Cremophor RH40 and Capryol 90. Transcutol HP was found to exhibit maximum emulsification ability amongst all the cosurfactants tried. Finally, Based on the results of preliminary screening of both IRB and OLM, a distinct system was selected consisting of Capryol 90 as oily phase, Cremophor RH40 as surfactant and Transcutol HP as the cosurfactant and detailed study of the system was performed using pseudo ternary phase diagram.

**Table 3: Emulsification efficiency of various cosurfactants**

Cosurfactants	% Transmittance*	No. of inversions
PEG 200	99.33±0.38	5
PEG 400	99.53±0.12	4
PEG 600	94.43±0.15	4
Transcutol HP	99.83±0.06	3
Propylene glycol	98.80±0.26	7
Glycerol	99.20±0.10	15

\*Values are expressed as mean±SD, n=3

### Construction of pseudo ternary phase diagram

Pseudoternary phase diagrams were constructed to identify the nanoemulsion region and optimize the concentration of the selected vehicles. Components used for the construction of pseudo ternary phase diagram are Capryol 90 (oil phase), Cremophor RH 40 (surfactant), Transcutol HP (cosurfactant) and distilled water (aqueous phase). The nanoemulsion phase was identified as the area where clear and transparent formulae were obtained on dilutions based on visual inspection of samples. The size of the nanoemulsion region in the diagrams was compared, the larger the size the greater the self-nano emulsification efficiency. Pseudoternary phase diagrams showed that the zone of nanoemulsion (the grayish area) was largest in formulae prepared with Cremophor RH 40-Transcutol HP mixture (Smix) at 1:1 ratio as shown in fig. (9-14). Thus, fixing the surfactant/cosurfactant ratio at 1:1 is a better choice from the stability point of view [33]. At Smix 1:1, and when cosurfactant was added with

surfactant in equal amounts, a higher nanoemulsion region was observed, perhaps because of the further reduction of the interfacial tension and increased the fluidity of the interface at Smix 1:1.

### Characterization and Evaluation of unloaded SNEDDS

#### Robustness to dilution

The ability of SNEDDS formulae to be diluted without any phase separation and drug precipitation is essential for its use as a drug delivery vehicle since, after administration, it will almost certainly be diluted by body fluids. After dilution of different SNEDDS formulae, the resulting nanoemulsions were found to remain clear, transparent and showed no phase separation even after 24 h as shown in table (4). This implied that these formulae were stable at infinite aqueous dilution. In addition, the composition and pH of the aqueous phase was found to have no effect on the properties of nanoemulsions [34].

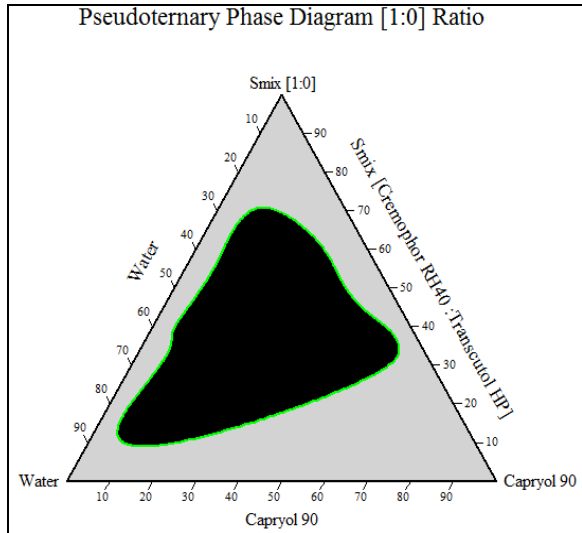


Fig. 9: Pseudo-ternary phase diagram of Smix [1:0]

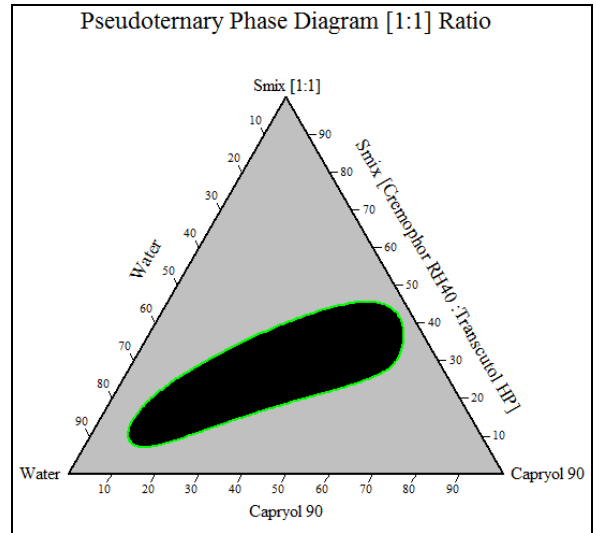


Fig. 10: Pseudo-ternary phase diagram of Smix [1:1]

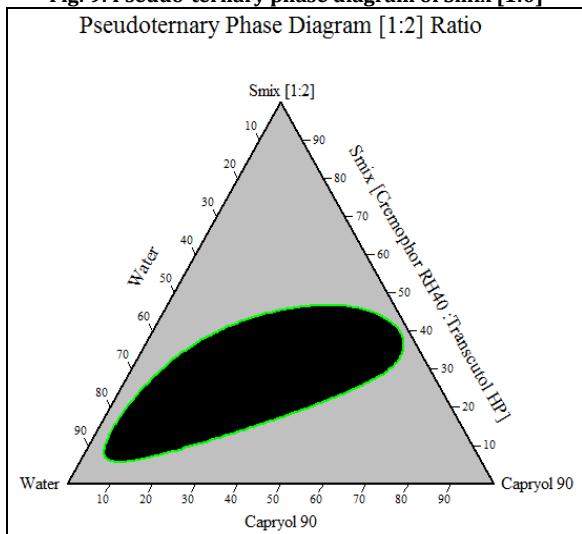


Fig. 11: Pseudo-ternary phase diagram of Smix [1:2]

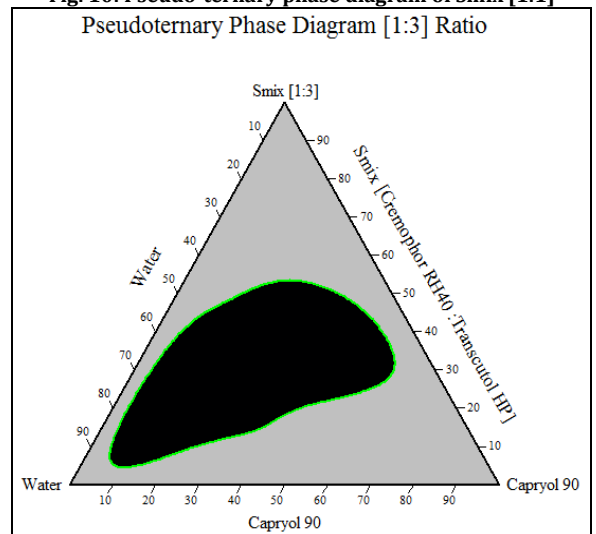


Fig. 12: Pseudo-ternary phase diagram of Smix [1:3]

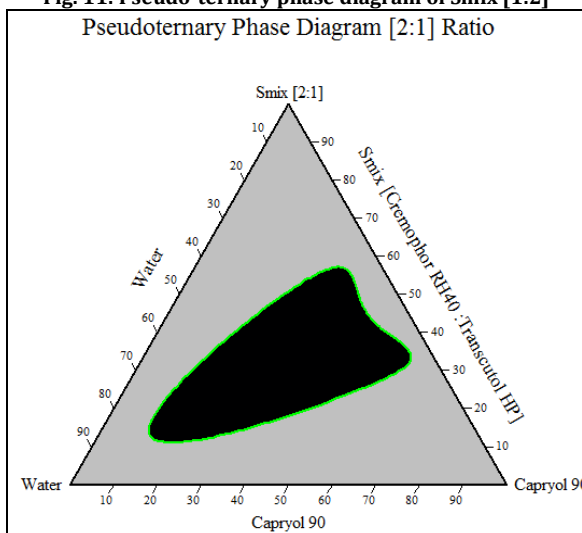


Fig. 13: Pseudo-ternary phase diagram of Smix [2:1]

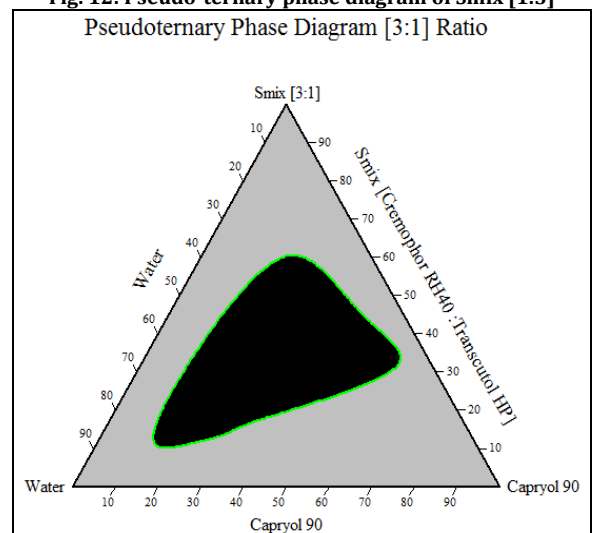


Fig. 14: Pseudo-ternary phase diagram of Smix [3:1]

**Thermodynamic stability studies**

All SNEDDS formulae showed no signs of precipitation, cloudiness or separation after heating-cooling cycles, centrifugation and freeze-thaw cycles. However, formulae F9 and F13 showed some turbidity

after freeze-thaw cycles. It indicates that as the concentration of oil increases with low concentration of Smix, the stability of the formula is decreased as the amount of surfactant required to emulsify the oil is not sufficient. The observations found during thermodynamic stability studies are given in table (5).

Table 4: Robustness to dilution results of various SNEDDS formulae

Formula	Distilled water			0.1 N HCL			Phosphate buffer pH 6.8		
	10	100	1000	10	100	1000	10	100	1000
F1	√	√	√	√	√	√	√	√	√
F2	√	√	√	√	√	√	√	√	√
F3	√	√	√	√	√	√	√	√	√
F4	√	√	√	√	√	√	√	√	√
F5	√	√	√	√	√	√	√	√	√
F6	√	√	√	√	√	√	√	√	√
F7	√	√	√	√	√	√	√	√	√
F8	√	√	√	√	√	√	√	√	√
F9	√	√	√	√	√	√	√	√	√
F10	√	√	√	√	√	√	√	√	√
F11	√	√	√	√	√	√	√	√	√
F12	√	√	√	√	√	√	√	√	√
F13	√	√	√	√	√	√	√	√	√
F14	√	√	√	√	√	√	√	√	√
F15	√	√	√	√	√	√	√	√	√
F16	√	√	√	√	√	√	√	√	√

Where (√) means stable formula which showed no phase separation or precipitation

Table 5: Thermodynamic stability studies of various SNEDDS formulae

Formula	Heating cooling cycles	Centrifugation test	Freeze thaw cycles
F1	√	√	√
F2	√	√	√
F3	√	√	√
F4	√	√	√
F5	√	√	√
F6	√	√	√
F7	√	√	√
F8	√	√	√
F9	√	√	x
F10	√	√	√
F11	√	√	√
F12	√	√	√
F13	√	√	x
F14	√	√	√
F15	√	√	√
F16	√	√	√

Where (√) indicates the formula passed the test and (x) indicates the formula failed the test

Table 6: Visual observations of dispersibility test for various SNEDDS formulae

Formula	Observations	Grade
F1	Rapidly forming clear emulsion	A
F2	Rapidly forming clear emulsion	A
F3	Rapidly forming clear emulsion	A
F4	Rapidly forming clear emulsion	A
F5	Rapidly forming clear emulsion	A
F6	Rapidly forming clear emulsion	A
F7	Rapidly forming clear emulsion	A
F8	Rapidly forming clear emulsion	A
F9	Rapidly forming, slightly less clear emulsion	B
F10	Rapidly forming clear emulsion	A
F11	Rapidly forming clear emulsion	A
F12	Rapidly forming clear emulsion	A
F13	Rapidly forming, slightly less clear emulsion	B
F14	Rapidly forming, slightly less clear emulsion	B
F15	Rapidly forming clear emulsion	A
F16	Rapidly forming clear emulsion	A

#### Assessment of efficiency of self-emulsification (Dispersibility test)

The *in-vitro* performances of the formulae were visually assessed using the grading system previously mentioned and the results were shown in the table (6). Among the sixteen self-emulsified compositions, 13 formulae were found to be grade A. However formulae (F9, F13 and F14) were categorized under grade B due to their high oil and low Smix compositions

#### Self-emulsification time

The rate of emulsification is an important index for the assessment of the efficiency of emulsification. Since the free energy required to form a nanoemulsion is very low, the formation is thermodynamically spontaneous. The SNEDDS should disperse completely and quickly when subjected to aqueous dilution under mild agitation. The recorded self-emulsification times for the sixteen tested formulae are

represented in table (7). From the results obtained, it was evident that all the tested formulae were self-emulsified within  $8 \pm 1.53$  to  $23 \pm 2.31$  seconds. The results revealed that self-emulsification time depends mainly upon the individual composition and its proportion of oil, surfactant and cosurfactant. The results showed that as the concentration of surfactant increases, the spontaneity of emulsification process increased and self-emulsification time decreases. This may be due to the capacity of Cremophor RH 40 in reducing the interfacial tension, and thus excess diffusion of aqueous phase into the oil occurs causing significant interfacial disruption and discharge of droplet into the bulk aqueous phase [35].

**Viscosity determination**

Viscosity studies are necessary for SNEDDS to characterize the system physically and to control its stability. The viscosity of SNEDDS is critical during their dispersion in the aqueous phase. Higher viscosities tend to slow down the emulsification rate which may affect *in-vivo* drug release and bioavailability profiles. From viscosity determination results, it was observed that as the concentration of oil and Smix increased the viscosity of SNEDDS formulae also get increased as shown in fig. (15). The SNEDDS formulae had the average viscosity range between  $16.54 \pm 0.73$  cps

and  $64.40 \pm 0.61$  cps. However after dilution with 100 times distilled water, the viscosity range decrease and became between  $3.84 \pm 0.98$  cps and  $34.95 \pm 0.64$  cps. All formulae were found to have rather low viscosities which indicated the resulted nanoemulsion to be O/W type. The viscosity values recorded by the SNEDDS formulae in the present study were low enough to preclude the possibility of rapid self-emulsification [36].

**Spectroscopic characterization of optical clarity**

The percentage transmittance (%T) is an important parameter to determine the isotropic nature of the system. A value of %T closer to 100% signified that all of the selected formulae were clear, transparent and globules size in the nanometric range, which in turn indicates that the formula has a large surface area for drug release, high capacity to undergo enhanced absorption in biological matrix and thus have ability for increased oral bioavailability. Higher transmittance should be obtained with optically clear solutions, since cloudier solutions will scatter more of the incident radiation, resulting in lower transmittance. On 100 fold dilution, the percentage transmittance of SNEDDS formulae was found to be in the range of 93.33 % to 99.77 % as presented in table (7) which confirms good transparent nature of all SNEDDS formulae.

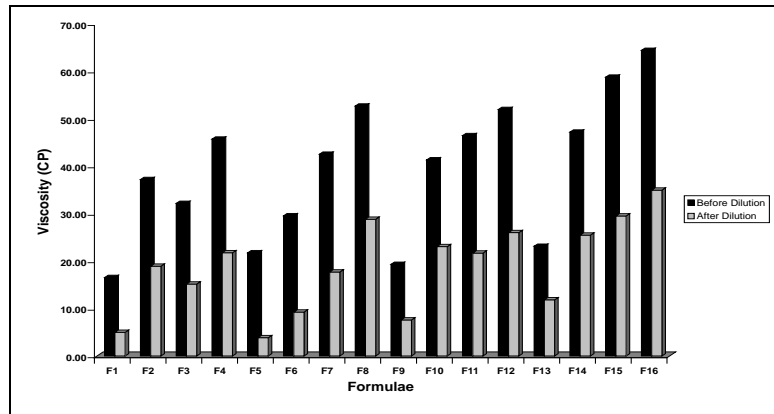


Fig. 15: Plot of viscosity before and after dilution for various SNEDDS formulae

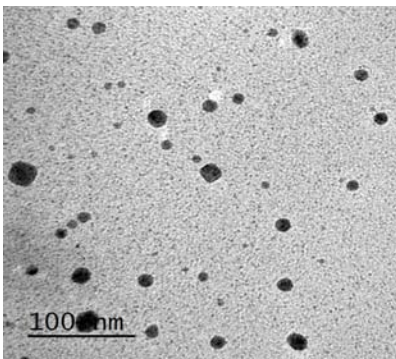


Fig. 16: TEM photograph of F1

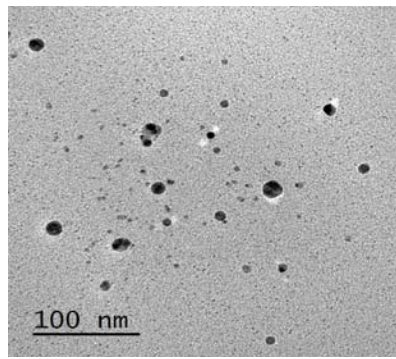


Fig. 17: TEM photograph of F2

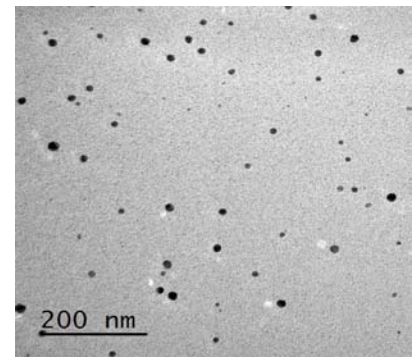


Fig. 18: TEM photograph of F3

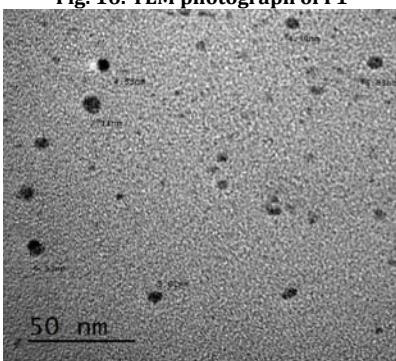


Fig. 19: TEM photograph of F4

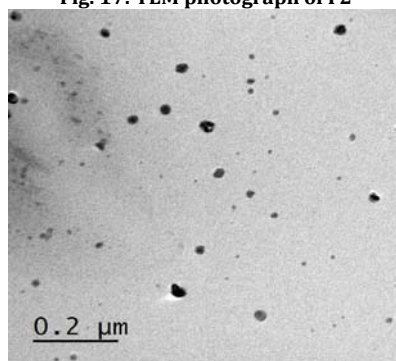


Fig. 20: TEM photograph of F5

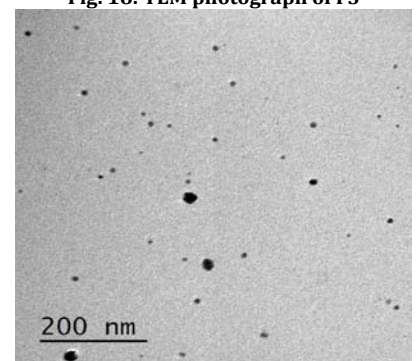


Fig. 21: TEM photograph of F6

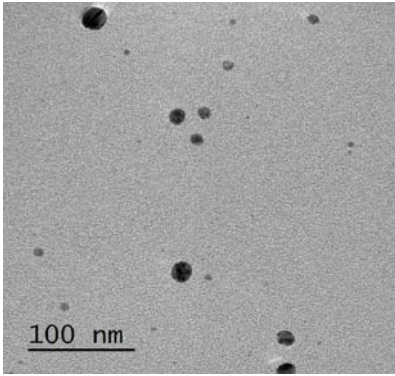


Fig. 22: TEM photograph of F7

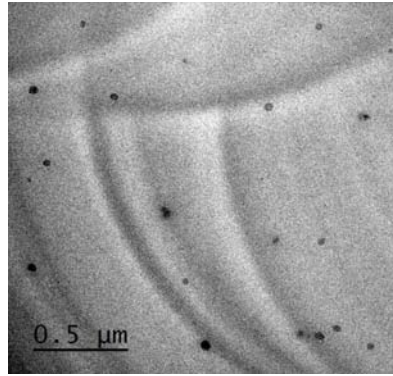


Fig. 23: TEM photograph of F8

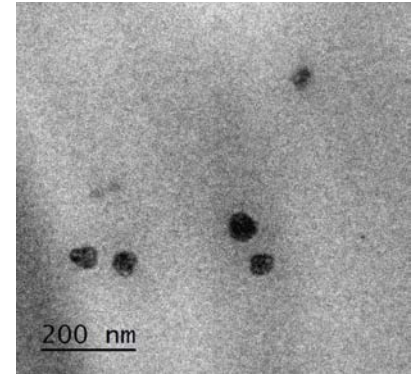


Fig. 24: TEM photograph of F9

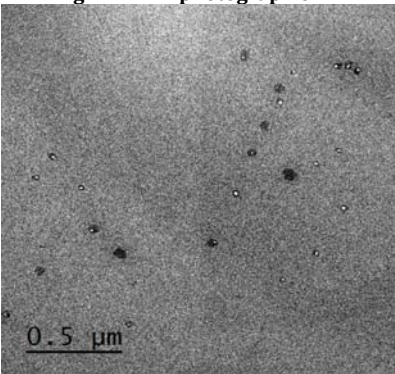


Fig. 25: TEM photograph of F10

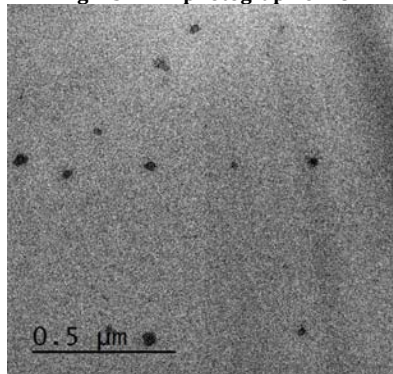


Fig. 26: TEM photograph of F11

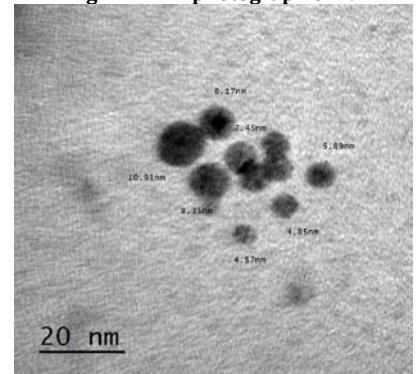


Fig. 27: TEM photograph of F12

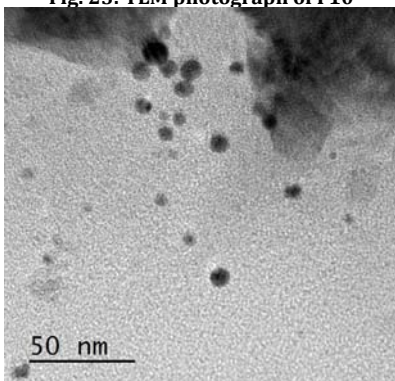


Fig. 28: TEM photograph of F13

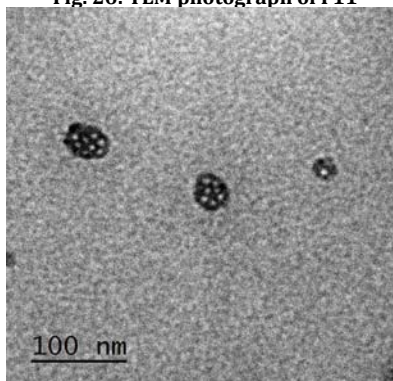


Fig. 29: TEM photograph of F14

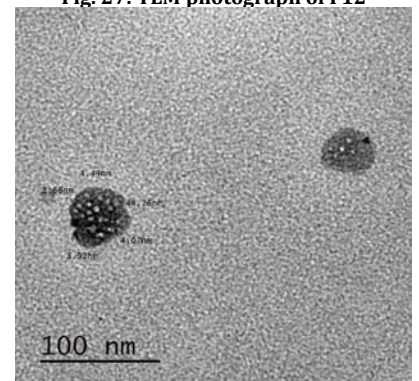


Fig. 30: TEM photograph of F15

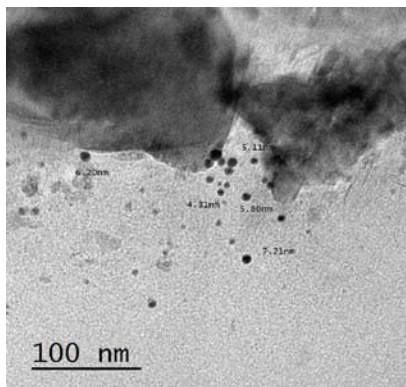


Fig. 31: TEM photograph of F16

**Transmission electron microscopy (TEM)**

TEM photographs of unloaded SNEDDS formulae subsequent to post dilution with distilled water are shown in fig. (16-31) and interpreted for surface morphology and globule size. From the

presented figures, it was apparent that globules of all formulae were well dispersed and no globule aggregation took place. TEM analysis revealed the formation of spherical and homogeneous droplets with a size smaller than 50 nm, which satisfies the criteria of nanometric size range required for nanoemulsifying formulae [37].

**Droplet size analysis and polydispersibility Index (PDI) determination**

The droplet size is the crucial factor in the SNEDDS performance because it determines the rate and extent of drug release as well as drug absorption. Moreover, it has been reported that the smaller the particle size, the larger the interfacial surface area which may lead to more rapid absorption and improve the bioavailability. Systems with mean droplet size below 200 nm fulfill the criteria of SNEDDS. From droplet size analysis it was observed that SNEDDS formulae had the mean particle size in the range of 16.49 to 97.84 nm indicating their efficiency as SNEDDS as shown in fig. (32-47). It was also noticed that as the surfactant percentage increased, the mean droplet size decreased [38]. Furthermore, the droplet size increased when the concentration of lipid added increased from 5% to 15% due to the simultaneous decrease in the  $S_{mix}$  proportions [39]. The decrease in droplet size may be due to more surfactant being available for adsorption and the formation of a more closely packed surfactant film at the oil-water interface, thereby providing stable and

condense interfacial film, as well as the low interfacial tension in the system [40]. The mean droplet size is not the only parameter to be considered in the formulation of SNEDDS. The droplet size distribution is another parameter of equal importance. The droplet size distribution is expressed by a dimensionless value called the polydispersity index (PDI) which is the measure of particle

homogeneity and it varies from 0.0 to 1.0. The closer to zero the PDI value, the more homogenous are the particles. The small values of PDI shown by all SNEDDS formulae (0.076-0.431) indicate homogenous droplet population and narrow globule size distribution. This in turn indicates more uniform emulsions with higher physical stability.

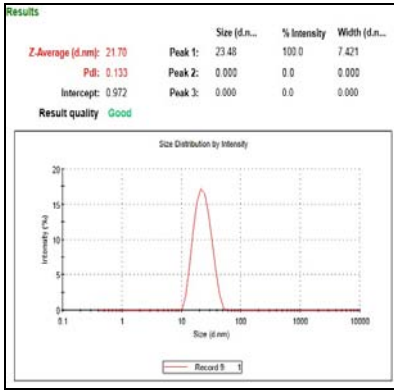


Fig. 32: Droplet size analysis of F1

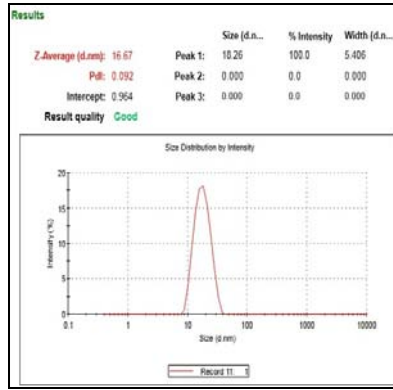


Fig. 33: Droplet size analysis of F2

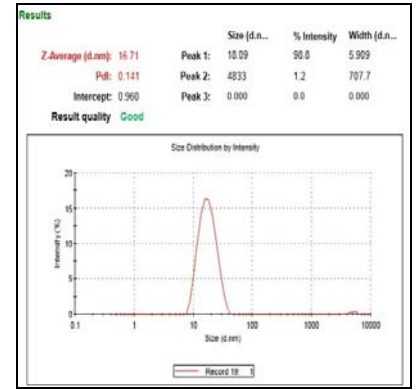


Fig. 34: Droplet size analysis of F3

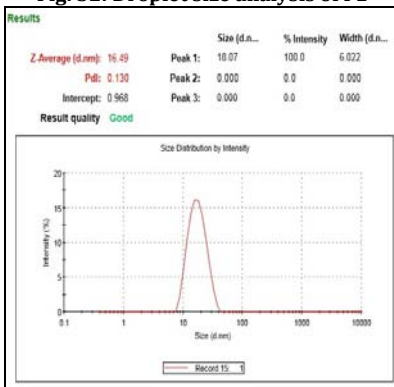


Fig. 35: Droplet size analysis of F4

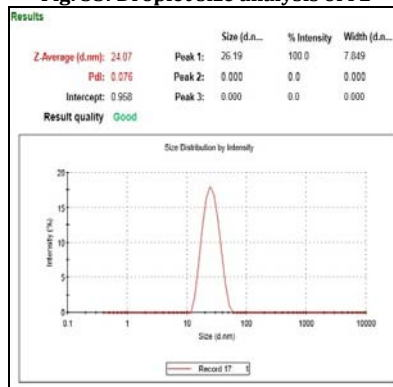


Fig. 36: Droplet size analysis of F5

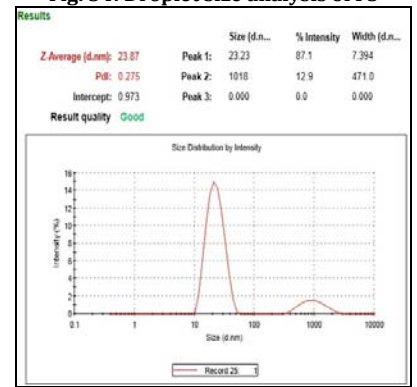


Fig. 37: Droplet size analysis of F6

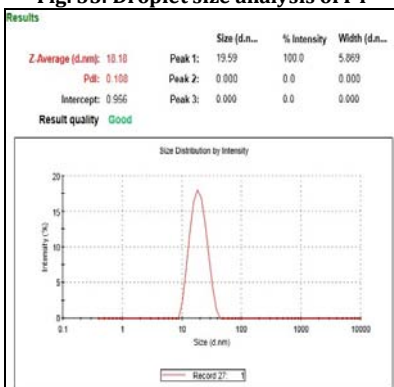


Fig. 38: Droplet size analysis of F7

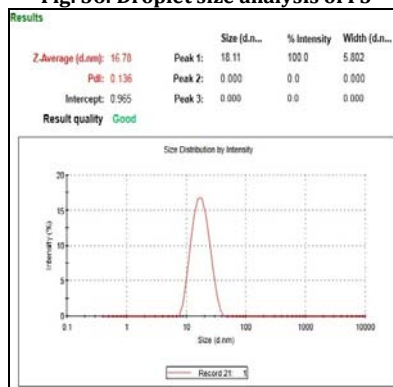


Fig. 39: Droplet size analysis of F8

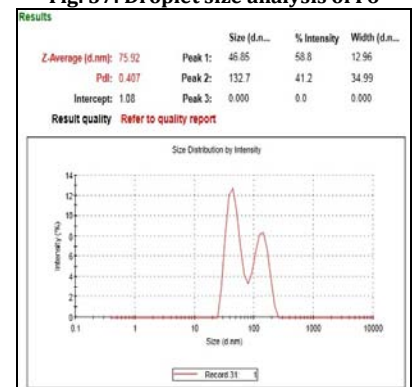


Fig. 40: Droplet size analysis of F9

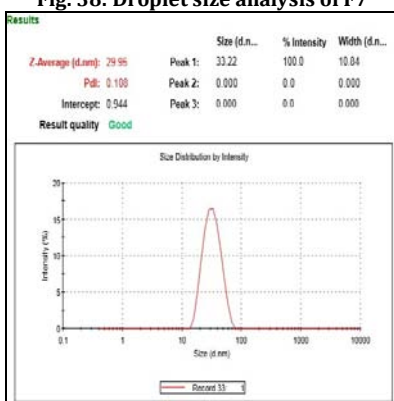


Fig. 41: Droplet size analysis of F10

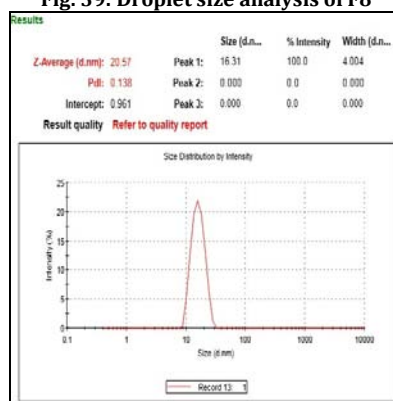


Fig. 42: Droplet size analysis of F11

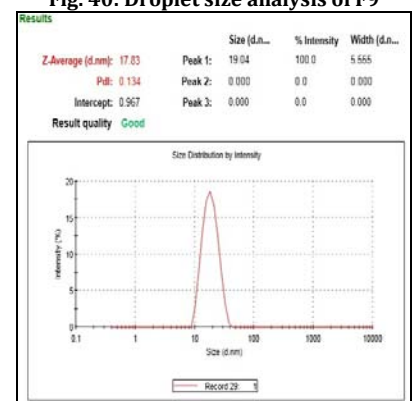


Fig. 43: Droplet size analysis of F12

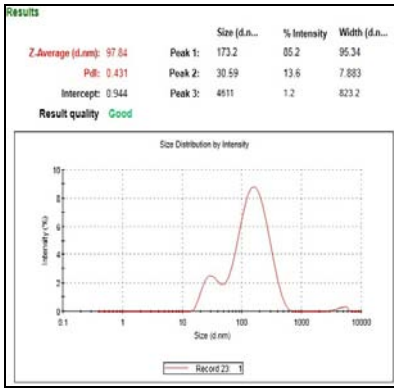


Fig. 44: Droplet size analysis of F13

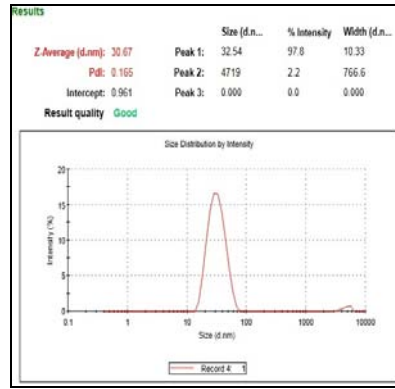


Fig. 45: Droplet size analysis of F14

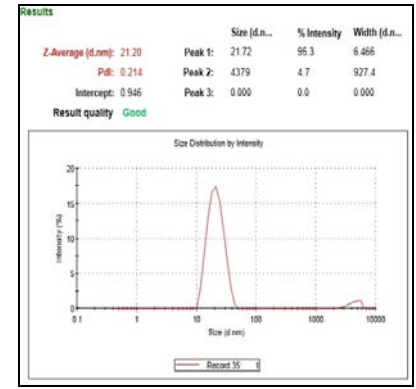


Fig. 46: Droplet size analysis of F15

Table 7: Self-emulsification time, % transmittance and zeta potential of SNEDDS formulae

Formula	Self-emulsification time* (Sec.)	% Transmittance*	Zeta potential (mV)
F1	15±0.58	99.53±0.21	-5.86
F2	17±2.00	99.67±0.06	-3.75
F3	10±1.00	99.50±0.20	-2.71
F4	8±1.53	99.77±0.23	-4.98
F5	21±2.08	98.70±0.20	-5.84
F6	20±1.15	98.63±0.21	-2.96
F7	15±1.53	98.90±0.17	-3.43
F8	12±0.58	99.10±0.26	-4.10
F9	19±1.73	94.60±0.30	-2.12
F10	21±1.00	98.13±0.25	-5.45
F11	18±1.15	98.60±0.17	-8.55
F12	14±2.08	99.03±0.12	-5.21
F13	23±2.31	93.33±0.51	-1.94
F14	17±1.53	97.60±0.26	-3.39
F15	20±1.73	98.07±0.15	-2.92
F16	16±1.00	98.57±0.06	-2.56

\*Values are expressed as mean±SD, n=3

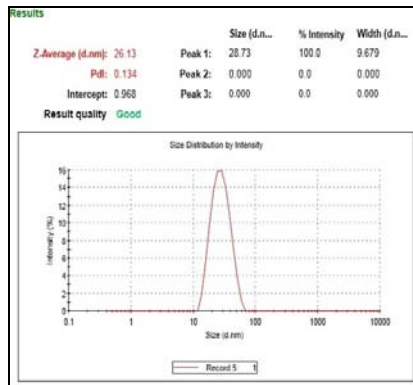


Fig. 47: Droplet size analysis of F16

**Zeta potential determination**

The zeta potential values of prepared SNEDDS formulae listed in table (7). The results were in the range of -1.94 to -8.55 mV. Negative values of zeta potential of all formulae give indication of stable systems [41]. Our results were in complete accordance with Maulik et al. who prepared stable SMEDDS lovastatin oral formulations, and found that Zeta potential of all SNEDDS formulation was found between -0.228 to -10.7 mV, that may be due to that formulation consist of non-ionic components which show relatively neutral charge and not affected by body membrane charge during absorption [42].

**CONCLUSION**

The unloaded systems were found to fulfill the criteria of adequate SNEDDS. They had rapid self-emulsification time, adequate mean

globule size (<100 nm), good dispersion characteristics (PDI values <0.5) as well as marked stability on dilution. The study concludes that the prepared self emulsified prototype was ready to incorporate many poorly soluble drugs in order to improve their solubility as well as bioavailability profile. Accordingly, SNEDDS are promising carriers for the oral delivery of both IRB and OLM aiming to solve their major oral delivery problem which is first-pass metabolism. Formulae with the smallest particle size, lowest emulsification time, best optical clarity and robust to dilution and pH change were selected to be loaded with IRB and OLM for further study.

**CONFLICTS OF INTERESTS**

The authors declare no conflict of interest

**REFERENCES**

1. Wang Z, Sun J, Wang Y, Liu X, Liu Y, Fu Q. Preparation and *in vitro/in vivo* evaluation of solid self-emulsifying nitrendipine pellets. Int J Pharm 2010;383:1-6.
2. Ratnam DV, Chandraiah G, Meena AK, Ramarao P, Kumar MN. The co-encapsulated antioxidant nanoparticles of ellagic acid and coenzyme Q10 ameliorate hyperlipidemia in high fat diet fed rats. J Nanosci Nanotechnol 2009;9:6741-6.
3. Shen H, Zhong M. Preparation and evaluation of self-microemulsifying drug delivery systems (SMEDDS) containing atorvastatin. J Pharm Pharmacol 2006;58:1183-91.
4. Anuradha S, Pratikkumar A, Darshana H. Peppermint oil based drug delivery system of aceclofenac with improved anti-inflammatory activity and reduced ulcerogenicity. Int J Pharma Biosci Technol 2013;1:89-101.
5. Pouton CW. Lipid formulations for oral administration of drugs: non-emulsifying, self-emulsifying and self-microemulsifying drug delivery systems. Eur J Pharm Sci 2000;11:93-8.

6. Ashok K, Kuldeep S, Murugesh K, Sriram R, Ramesh M. Formulation and development of an albendazole self-emulsifying drug delivery system (SEDDS) with enhanced systemic exposure. *Acta Pharm* 2012;62:563-80.
7. Kommuru T, Gurley B, Khan M, Reddy I. Formulation, development and bioavailability assessment of self-emulsifying drug delivery systems (SEDDS) of coenzyme Q10. *Int J Pharm* 2001;212:233-46.
8. Kale A, Patravale V. Design and evaluation of self-emulsifying drug delivery systems (SEDDS) of nimodipine. *AAPS PharmSciTech* 2008;9:191-6.
9. Kishanta K, Uma S, Subasini P, Debananda M, Ghanshyam P, Kanhu C. Method development, validation and stability study of irbesartan in bulk and pharmaceutical dosage form by UV-spectrophotometric method. *Int J Pharm Biol Arch* 2011;2:1114-22.
10. Prabhakar K, Vipan K, Sudhir R. Spectrophotometric estimation of olmesartan medoxomil in tablet dosage form with stability studies. *Int J Chem Tech Res* 2010;2:1129-34.
11. Patel J, Patel A, Raval M, Sheth N. Formulation and development of a self-nanoemulsifying drug delivery system of irbesartan. *J Adv Pharm Tech Res* 2011;2:9-16.
12. Nakagomi R, Nakai D, Kawai K, Yoshigae Y, Tokui T, Abe T, *et al.* Hepatobiliary transport of olmesartan, A novel angiotensin II blocker. *Drug Metab Dispos* 2006;34:862-9.
13. Dixit R, Nagarsenker M. Design, optimization and evaluation of self-nanoemulsifying granules of ezetimibe. *Eur J Pharm Sci* 2008;35:92-183.
14. Srinivas C, Sagar S. Enhancing the bioavailability of simvastatin using micro emulsion drug delivery system. *Asian J Pharm Clin Res* 2012;5:134-9.
15. Date A, Nagarsenker M. Design and evaluation of self-nanoemulsifying drug delivery systems (SNEEDS) for cefpodoxime proxetil. *Int J Pharm* 2007;329:166-72.
16. Patel A, Vavia P. Preparation and *in vivo* evaluation of SMEDDS (self-microemulsifying drug delivery system) containing fenofibrate. *AAPS J* 2007;9:344-52.
17. Divyakumar B, Priyanka B, Kiran B. Formulation and evaluation of self microemulsifying drug delivery system of low solubility drug for enhanced solubility and dissolution. *Asian J Biomed Pharm Sci* 2012;2:7-14.
18. Sheikh S, Shakeel F, Talegaonkar S, Ahmad F, Khar R, Ali M. Development and bioavailability assessment of ramipril nanoemulsion formulation. *Eur J Pharm Biopharm* 2007;66:227-43.
19. Atef E, Belmonte A. Formulation, *in-vitro* and *in-vivo* characterization of phenytoin self-emulsifying drug delivery system. *Eur J Pharm Sci* 2008;35:257-63.
20. Ehab I, Saleh A, Ahmed M, Mansoor A. Preparation and *in-vitro* characterization of self-nanoemulsified drug delivery system (SNEEDS) of all-trans-retinol acetate. *Int J Pharm* 2004;285:109-19.
21. Nekkanti V, Karatgi P, Prabhu R, Pillai R. Solid self-microemulsifying formulation for candesartan cilexetil. *AAPS PharmSciTech* 2010;11:9-17.
22. Chopade V, Chaudhari P. Development and evaluation of self-emulsifying drug delivery system for lornoxicam. *Int J Res Dev Pharm Life Sci* 2013;2:531-7.
23. Khoo S, Humberstone A, Porter C, Edwards G, Charman W. Formulation, design and bioavailability assessment of lipidic self-emulsifying formulations of halofantrine. *Int J Pharm* 1998;167:155-64.
24. Balakrishnan P, Lee B, Oh D, Kim J, Hong M, Jee JP, *et al.* Enhanced oral bioavailability of coenzyme Q10 by a novel solid self-emulsifying drug delivery system. *Int J Pharm* 2009;374:66-72.
25. Ghosh P, Majithiya R, Umrethia M, Murthy S. Design and development of microemulsion drug delivery system of acyclovir for improvement of oral bioavailability. *AAPS PharmSciTech* 2006;7:172-7.
26. Balakrishnan P, Lee J, Oh D. Enhanced oral bioavailability of dexibuprofen by a novel solid self-emulsifying drug delivery system (SEDDS). *Eur J Pharm Biopharm* 2009;72:539-45.
27. Zakia B, Suyang Z, Wenli Z, Junlin W. Formulation, development and bioavailability evaluation of a self-nanoemulsifying drug delivery system (SNEEDS) of atorvastatin calcium. *Int J Pharm* 2013;29:1103-13.
28. Arpan C, Vineetkumar P, Manish N, Kamala V, Chamanlal S. A novel lipid-based oral drug delivery system of nevirapine. *Int J PharmTech Res* 2011;3:1159-68.
29. Humberstone A, Charman W. Lipid based vehicles for oral delivery of poorly water soluble drugs. *Adv Drug Delivery Rev* 2008;25:103-28.
30. Urvashi G, Ritika A, Geeta A. Formulation, design and evaluation of a self-microemulsifying drug delivery system of lovastatin. *Acta Pharm* 2012;62:357-70.
31. Farinato R, Rowell R. Optical properties of emulsions. *Encyclopedia of emulsion technology*, Marcel Dekker, New York; 2000;1:439-79.
32. Chen M. Lipid excipients and delivery systems for pharmaceutical development: a regulatory perspective. *Adv Drug Delivery Rev* 2008;60:768-75.
33. Spornath A, Yagmur A, Aserin A, Hoffman R, Garti N. Food-grade microemulsions based on nonionic emulsifiers: media to enhance lycopene solubilization. *J Agric Food Chem* 2002;50:6917-22.
34. Li P, Ghosh A, Wagner R, Krill S, Joshi Y. Effect of combined use of nonionic surfactant on formation of oil-in-water microemulsions. *Int J Pharm* 2005;288:27-34.
35. Kallakunta V, Bandari S, Jukanti R, Veerareddy P. Formulation and evaluation of oral self-emulsifying powder of lercanidipine hydrochloride. *Powder Technol* 2012;221:375-82.
36. Sharma B, Sharma A, Arora S, Gupta S, Bishnoi M. Formulation, optimization and evaluation of novel nanoemulsion formulations for transdermal potential of celecoxib. *Acta Pharm* 2007;57:315-23.
37. Wu X, Xu J, Huang X, Wen C. Self-microemulsifying drug delivery system improves curcumin dissolution and bioavailability. *Drug Dev Ind Pharm* 2011;37:15-23.
38. Nazzal S, Nutan M, Palamakula A, Shah R, Zaghoul A, Khan M. Optimization of a self-nanoemulsified tablet dosage form of ubiquinone using response surface methodology: effect of formulation ingredients. *Int J Pharm* 2002;240:103-14.
39. Hong J, Kim J, Song Y, Park J, Kim C. A new self-emulsifying formulation of itraconazole with improved dissolution and oral absorption. *J Controlled Release* 2006;110:332-8.
40. Cui Y, Li L, Gu J, Zhang T, Zhang L. Investigation of microemulsion system for transdermal delivery of ligustrazine phosphate. *Afr J Pharm Pharmacol* 2011;5:1674-81.
41. Rai S, Yasir M. Preparation, optimization and *in-vitro* evaluation of cinnarizine loaded lipid based system. *IOSR J Pharm* 2012;2:47-56.
42. Maulik J, Natvarlal M, Ritesh B, Rakesh P. Formulation and evaluation of self-microemulsifying drug delivery system of lovastatin. *Self-Microemulsion Lovastatin/Asian J Pharm Sci* 2010;5:266-75.